ACS Chemical Neuroscience

pubs.acs.org/chemneuro

Research Article

# Neurotropic activity and safety of methylene-cycloalkylacetate (MCA) derivative 3-(3-allyl-2-methylenecyclohexyl) propanoic acid

Adi Lahiani, Dikla Haham-Geula, David Lankri, Susan Cornell-Kennon, Erik M. Schaefer, Dmitry Tsvelikhovsky,* and Philip Lazarovici*

Cite This: *ACS Chem. Neurosci.* 2020, 11, 2577−2589

Read Online

ACCESS | Metrics & More | Article Recommendations | Supporting Information

**ABSTRACT:** Polyneuropathy is a disease involving multiple peripheral nerves injuries. Axon regrowth remains the major prerequisite for plasticity, regeneration, circuit formation, and eventually functional recovery and therefore, regulation of neurite outgrowth might be a candidate for treating polyneuropathies. In a recent study, we synthesized and established the methylene-cycloalkylacetate (MCAs) pharmacophore as a lead for the development of a neurotropic drug (inducing neurite/axonal outgrowth) using the PC12 neuronal model. In the present study we extended the characterizations of the in vitro neurotropic effect of the derivative 3-(3-allyl-2-methylenecyclohexyl) propanoic acid (MCA-13) on dorsal root ganglia and spinal cord neuronal cultures and analyzed its safety properties using blood biochemistry and cell counting, acute toxicity evaluation in mice and different in vitro "off-target" pharmacological evaluations. This MCA derivative deserves further preclinical mechanistic pharmacological characterizations including therapeutic efficacy in in vivo animal models of polyneuropathies, toward development of a clinically relevant neurotropic drug.

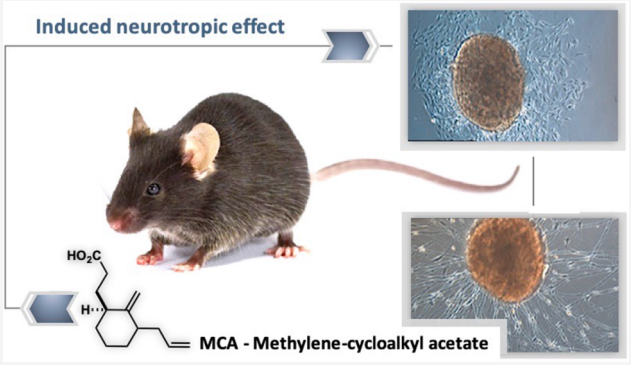


**KEYWORDS:** *Methylene-cycloalkylacetate, neurotropic activity, safety, off-target, GPCR, transporter, enzyme, $PGE_2$, kinome, PC12, DRG, spinal cord neuron*

## 1. INTRODUCTION

Polyneuropathy is a disease involving multiple peripheral nerves injuries, which affects nerves responsible for pain, movement, or both. It may also affect the autonomic nerves responsible for controlling functions such as digestion, bladder activity, blood pressure and heart rate.[1] The National Institute of Neurological Disorders and Stroke, NIH, USA estimates that approximately 20 million people in the United States have some form of peripheral neuropathy.[2] Clinically, neuropathy can arise from nerve partial or complete Wallerian axonal degeneration which is also a common feature of traumatic, ischemic, inflammatory, toxic, metabolic, genetic, and neuro-degenerative disorders affecting the central and the peripheral nervous system, leading to failure of nerve conduction and neural functions.[3] Nonetheless, the most commonly used agents for neuropathic pain treatment include tricyclic antidepressants, anticonvulsants, and serotonin-norepinephrine reuptake inhibitors.[4] To date, not a single drug can be found in the clinic that can stop or reverse the nerve injury or degeneration. Moreover, to the best of our knowledge, there are no drugs, which promote nerve regeneration.[5] A major weaknesses of an existing polyneuropathic drug development program is the inaccurate choice of a neuronal cellular target. In many polyneuropathies, there is very little, if any, death of the neuronal cell body. The primary acute pathology is distal axonal injury and degeneration. Yet, most high-throughput cell free, target drug-based screens use neuronal molecular targets and signaling molecules[6] and fail to take in consideration the phenotypic induction, or enhancement of new axonal sprouts which can reestablish the nerve circuit.

Neuroregeneration is a concept, which encompasses neuronal growth-promoting and inhibitory cues, leading to neuroplasticity and axonal outgrowth.[7] The principal morphological characteristics of neuritogenesis are branching of neurites followed by elongation of axons and dendritic arborization.[8] It has become apparent that damaged neurons do regenerate in an active process by different mechanisms under treatment with neurotrophins such as nerve growth factor (NGF)[9] and brain derived neurotrophic factor (BDNF).[10] Neuritogenic

**Received:** April 29, 2020
**Accepted:** July 15, 2020
**Published:** July 15, 2020

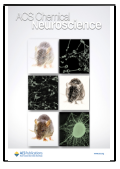







https://dx.doi.org/10.1021/acschemneuro.0c00255
*ACS Chem. Neurosci.* 2020, 11, 2577−2589

**Scheme 1. Synthesis of MCA-13**

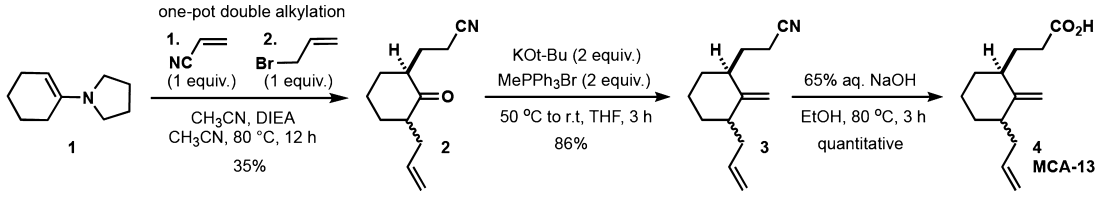


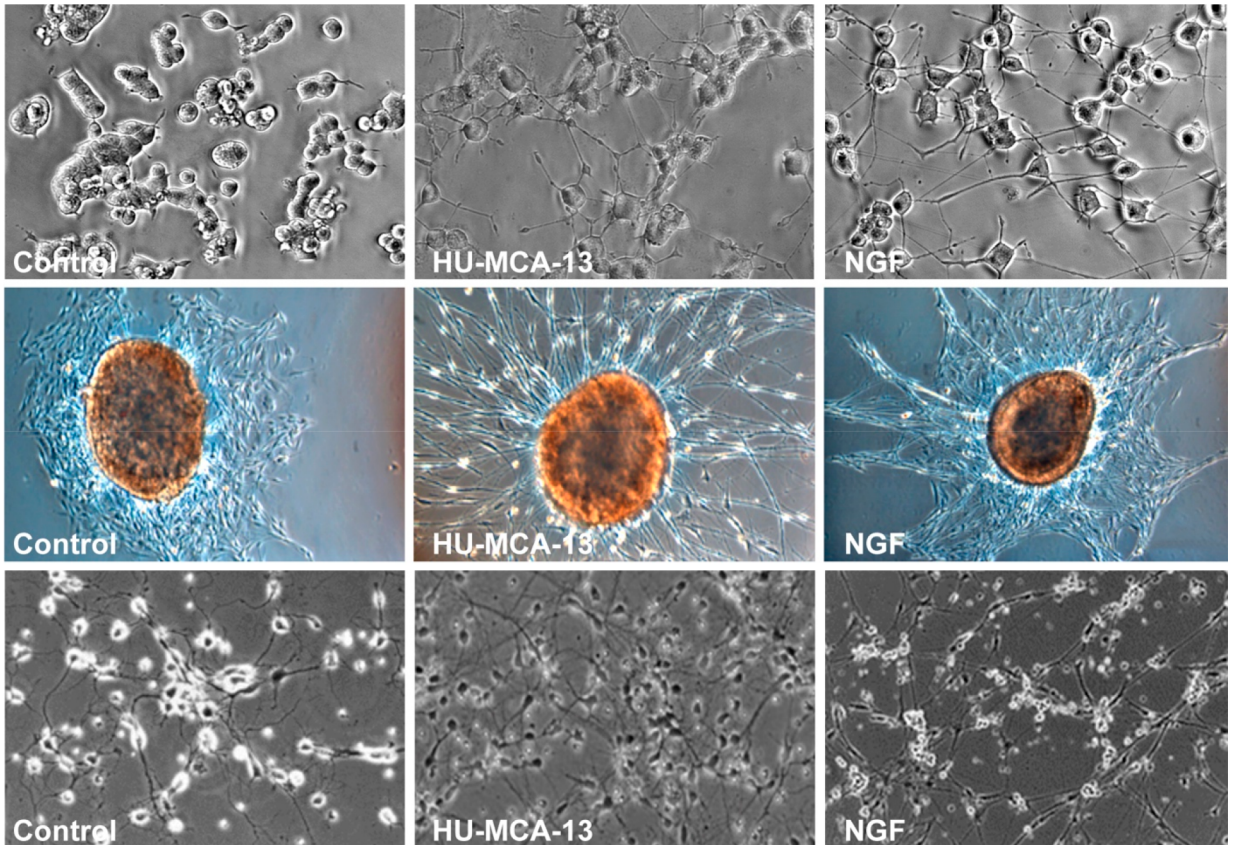


**Figure 1.** HU-**MCA-13 induced neurotropic effect in different neuronal cultures.** Neurotropic effect was measured after treatment with 5 $\mu$M of HU-MCA-13 of rat PC12 dopaminergic neurons (7 days, top row), mice dorsal root ganglion (DRG) explants (5 days, middle row) and rat spinal cord sensory neurons (14 days, bottom row). The negative control cultures were treated with 0.1% DMSO and the positive control cultures were treated with 50 ng/mL mouse $\beta$-nerve growth factor (NGF) for the same periods of time.

substances hold the promise of therapeutic efficacy in the treatment of neuronal injuries by the virtue of their ability to stimulate outgrowth of neurites from neuronal cells[11] which, cause a readjustment in the normal neuronal functions and local circuits in the damaged nervous system. Therefore, use of the neurotrophic factors seems to be an important step in the process of neuronal regeneration.[12] Many enhancers of nerve regeneration, such as stem cells[13] and neurotrophin growth factors[14] were found to enhance axonal regeneration after nerve injury in animal models and found safe and efficient in neuropathic therapy in placebo-controlled, randomized clinical trials,[15] but none has entered the clinic.[16] Most probably, the key reasons for this failure are the lengthy and costly regulatory process needed to evaluate complex biologicals for human use, the inability of neurotrophins to cross the blood-brain-barrier, the short-term survival of implanted stem cells, etc. To overcome this hurdle, use of natural and synthetic small molecules eliciting neuritogenic (neurotropic, neurite outgrowth) activity alone or in combination with neurotrophins (NGF, BDNF) is currently been focused as an alternative approach. Numerous agents have demonstrated the potential to enhance neuronal repair following spinal cord or peripheral nerve injury using neurite outgrowth as a biomarker for axonal extension in primary cell cultures and neuronal cell lines.[17] Recent drug discovery reports suggest that different synthetic compounds alone,[18] or in combination with neurotrophins, cooperate to induce the outgrowth of neurites in neurotrophic assays that identify molecules that stimulate differentiation-neurite outgrowth of neuronal cells,[19,17b] suggesting that synthetic molecules may harmonize very well for the treatment of neuronal polyneuropathies. Therefore, toward improving and accelerating drug development for nervous system disorders[20] there is a critical unmet clinical need for a safe drug that enhances peripheral nerve regeneration after injury or the dysfunction that results from polyneuropathies.

In a recent study, we reported the synthesis of an unique family of methylene-cycloalkylacetate (MCAs)-based small molecule, (often observed as scaffold of various compounds


https://dx.doi.org/10.1021/acschemneuro.0c00255
ACS Chem. Neurosci. 2020, 11, 2577−2589

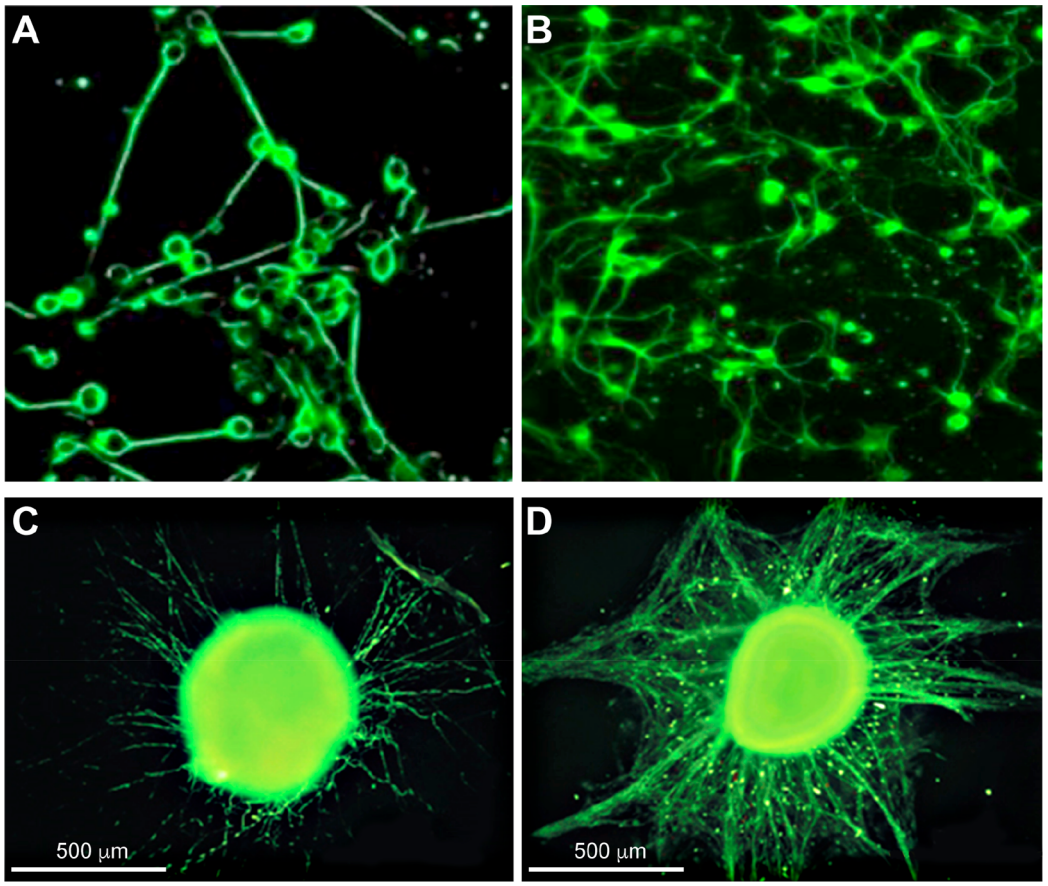


**Figure 2. HU-MCA-13 induced neurotropic effects in different neuronal cultures measured by immunofluorescence microscopy of expression of the axonal marker βIII tubulin. A** - PC12 neurons; **B** – spinal cord neurons; **C, D**- DRG explants. **A-C**- treatment with 5 μM HU-MCA-13 (like Figure 1); **D**-treatment with NGF (like Figure 1). βIII-tubulin was detected using an antineuron-specific βIII tubulin antibody.

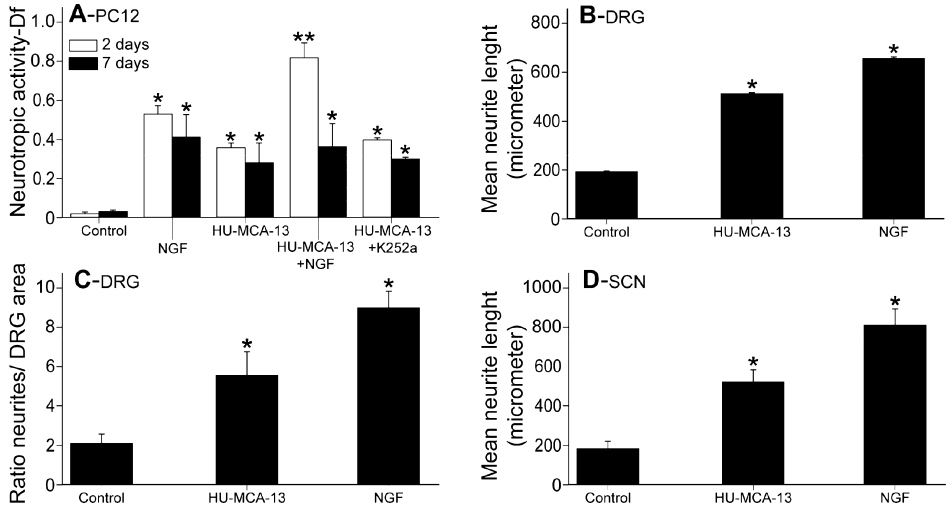


**Figure 3. Quantization of the neurotropic effect of HU-MCA-13.** The neurotropic effect was quantified from macroscopically micrographs according to two parameters: length of neurite outgrowth, as determined by either the Df parameter for PC12 cells (A) or measured with a micrometer scale for DRG (B) and spinal cord neurons (D) and the ratio between the neurites and DRG areas was calculated (C); PC12 cells were treated for 2 or 7 days, DRG explants were treated for 5 days and spinal cord neurons were treated for 14 days. Control cultures were treated with 0.1% DMSO; NGF, represents cultures treated with 50 ng/mL mouse βNGF; Data are means ± SD of at least 25 cells in three images each from three independent experiments. Statistical analysis was performed using one-way analysis of variance followed by Tukey's test. *$p < 0.01$ compared to control.

and drugs of natural origin) neurotropic drug (inducing neurite/axonal outgrowth) and indicated that the alkene element, integrated within the cycloalkylacetate core, was obligatory for the neurotropic activity.[21,22] Additional studies have led to a wide variety of potential pharmaceutical candidates that share the methylene-cycloalkylacetate (MCA)



https://dx.doi.org/10.1021/acschemneuro.0c00255
ACS Chem. Neurosci. 2020, 11, 2577−2589

scaffolds.[23] Present study further characterizes the neurotropic activities of these compounds, specifically a candidate labeled HU-MCA-13,[21] and analyzes its safety properties using blood biochemistry and cell counting, acute toxicity evaluation in mice and different in vitro "off-target" pharmacological evaluations. This MCA derivative deserves further preclinical mechanistic pharmacological characterizations and therapeutic efficacy in in vivo animal models of polyneuropathies toward development of a clinically relevant neurotropic drug.

## 2. RESULTS AND DISCUSSION

**Synthesis and chemical characterization of HU-MCA-13.** Based on recently reported protocol for general and collective syntheses of methylene-caycloalkyl acetates, the scaffold of HU-MCA-13 (Scheme 1) was successfully constructed through the simple and straightforward sequence of transformations: $\alpha,\alpha'$-double alkylation of 1-(cyclohex-1-en-1-yl)pyrrolidine **1**; olefination of ketone **2** (access to intermediate **3**); and hydrolysis (see section Materials and Methods).[21,24]

**Neurotropic activities of MCA-13.** *MCA-13 induced neurite outgrowth in PC12 dopaminergic cell cultures.* In the first step, using an established PC12 neurotropic in vitro assay, we confirmed the neurotropic effect of HU-MCA-13 (Figure 1, first row). Thereafter, by immunostaining, we found that cell bodies and neurite outgrowths of PC12 cells treated with 5 $\mu$M of HU-MCA-13 for 7 days expressed $\beta$ tubulin III (Figure 2A), a cytoskeletal protein which is specifically localized to neuronal microtubule network and its expression correlates with the earliest phases of neuronal differentiation.[25] Next, we investigated the neurite outgrowth enhancing effect of HU-MCA-13 when applied concomitantly with NGF, a known neurotrophin (Figure 3A). We found that HU-MCA-13 alone at 10 $\mu$M, enhanced neurite outgrowth to a $D_f$ value of 0.36 at 2 days and 0.30 at 7 days of treatment. NGF alone, at a regular dose of 50 ng/mL enhanced neurite outgrowth to a $D_f$ value of 0.54 at 2 days and 0.4 at 7 days of treatment (Figure 3A). To verify a possible additive or synergistic effect, we treated the cultures with a combination of low dose of NGF (1 ng/mL, generating 10% neurite outgrowth = $D_f$ of 0.05) and HU-MCA-13 (1 $\mu$M, generating about 10−15% neurite outgrowth = $D_f$ of 0.04), and found after 2 and 7 days of treatment, $D_f$ of 0.85 and 0.38 respectively, findings indicating a significant synergistic effect. Since NGF plays an important role during polyneuropathy inflammatory process,[26] this observation further strength the prediction of a potential synergistic enhancement regenerative effect of HU-MCA-13 upon in vivo delivery to an animal model of neuropathy. To verify whether NGF mediates HU-MCA-13 neurotropic effect by Trk A receptor, we pretreated the cultures with both 10 $\mu$M HU-MCA-13 and 250 nM K252a, a well-known Trk A inhibitor. Under these conditions, NGF neurotropic effect was abolished (data not shown) but not HU-MCA-13 induced neurotropic activity (Figure 3A). These findings may suggest that the neurotropic effect of HU-MCA-13 is not involving NGF-Trk A receptor signaling.

*HU-MCA-13 induced neurite outgrowth in dorsal root ganglion (DRG) sensory neurons.* In the second step, we study the effect of HU-MCA-13 on ex-vivo sensory neuronal cultures obtained from dissociated dorsal root ganglia (DRG), a model in which the neurons tend to extend neurites in culture at a high rate, and all neurite outgrowths are axons, as confirmed by immune staining for cytoskeletal-specific proteins.[27] The results indicated that in the control medium, there was very poor spontaneous neurite outgrowth of a length of about 200 $\mu$m (Figure 1 and Figure 3B) and a low ratio of 2 between the area covered by neurites and that covered by DRGs (Figure 3C). By contrast, NGF induced a strong, 3.5-fold increase in neurite outgrowth to a value of 700 $\mu$m (Figure 1 and Figure 3B) and a ratio of 8.5 between the area covered by neurites and that covered by the DRG ganglia (Figure 3C). Similarly, HU-MCA-13 induced a 2.5 fold increase in neurite outgrowth to a value of about 500 $\mu$m (Figure 1 and Figure 3B) and a ratio of 5.4 between the area covered by neurites and that covered by the DRG ganglia (Figure 3C). However, the neurite outgrowths induced by HU-MCA-13 were less mature than in NGF-treated ganglia as evident from their shorter length and the lower expression of the cytoskeletal-tubulin protein staining by comparison to NGF-treated DRGs (Figure 2 C compared to D). These findings may suggest that the maturation of the axons induced by HU-MCA-13 requires a longer period than for NGF, an issue deserving further experimentation. These experiments extend the neurotropic effect of MCA-13 observed with PC12 dopaminergic neuronal cultures to DRG sensory neurons.

*HU-MCA-13 induced neurite outgrowth in adult rat spinal cord primary cultures.* To study the effect of HU-MCA-13 on adult rat spinal cord primary cultures in vitro, we developed a purification procedure that yields enriched different types of spinal cord neuronal cultures. This neurotropic assay was performed using vehicle 1% DMSO in DMEM as control and 10 $\mu$M HU-MCA-13. The results in Figure 1 bottom row and Figure 3D clearly indicate that in control there was very poor spontaneous neurite outgrowth of a total length of about 180 $\mu$m and NGF induced neurite outgrowth to a total length of about 800 $\mu$m. Similarly, HU-MCA-13 induced a neurite outgrowth of 600 $\mu$m. Figure 2B indicates cytoskeletal-tubulin protein expression in the cultured neurons. These findings further extend the neurotropic effect of HU-MCA-13 to spinal cord neurons, in addition to DRGs and PC12 cells.

We also examined whether HU-MCA-13 would promote the survival of neurons from the spinal cord, by counting the number of neurons remaining after 48 h in culture. From our counts we estimated that 58 ± 10% of the neurons present at 3 h after plating survived for 48 h in the presence of HU-MCA-13, compared with only 35 ± 5% for neurons cultured without HU-MCA-13. While this result supports the conclusion that HU-MCA-13 increased in vitro the survival of a variety of different neuronal types within the spinal cord, present results do not exclude the possibility that certain types of spinal cord neurons might not respond to HU-MCA-13, or that some respond more than others do.

**Safety of HU-MCA-13.** *Single-dose, acute tolerance of HU-MCA-13 in mice.* This pilot study was conducted according to guidance for industry single dose acute toxicity testing for pharmaceuticals (https://www.fda.gov/regulatory-information/search-fda-guidance-documents/single-dose-acute-toxicity-testing-pharmaceuticals) to obtain acute information on the dose toxicity of HU-MCA-13 in male mice. Male C57BL/6 mice were injected intravenously with 0.2 mL of HU-MCA-13 in a dose of 250 mg/kg. Mice were monitored for the sensory-motor performance during the first week after injection using several routine motor tests, the neurologic function severity score (NSS) was measured, but no neurological losses were observed (Supporting Information,


https://dx.doi.org/10.1021/acschemneuro.0c00255
ACS Chem. Neurosci. 2020, 11, 2577−2589

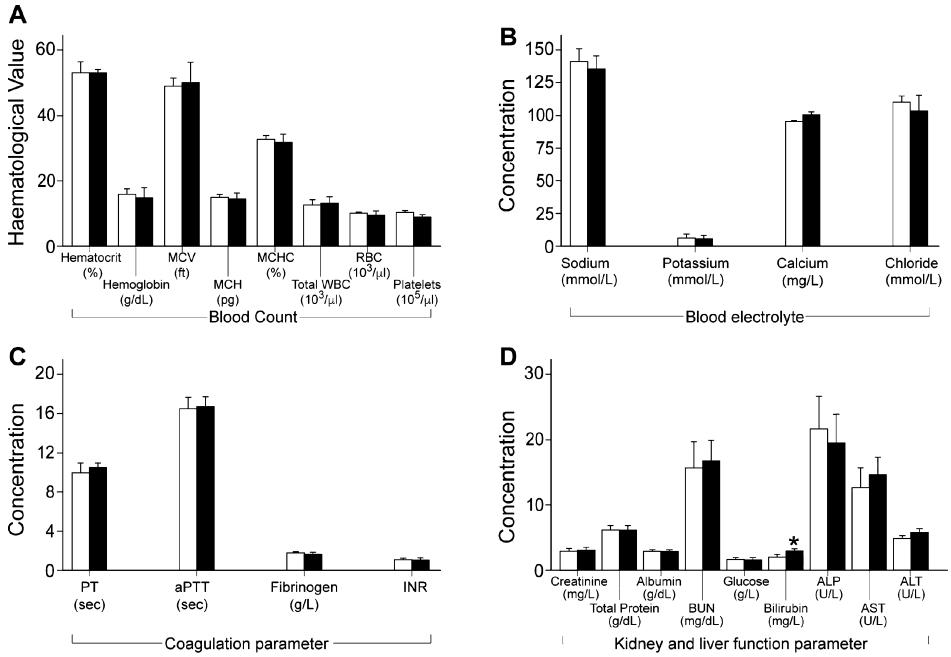


**Figure 4. Analysis of blood hematological and blood biochemistry parameters of HU-MCA-13-injected mice ($n$= 4, black) compared to DMSO treated group ($n$= 3; white); A.** Blood count; **B.** electrolytes; **C.** Coagulation; **D.** Kidney and liver functions. *$p$ < 0.01 compared to control; ALP; alkaline phosphatase; ALT, alanine transaminase; aPTT, activated partial thromboplastin time; AST, aspartate transaminase; BUN, blood urea nitrogen; INR, international normalized ratio; MCH, mean corpuscular hemoglobin; MCHC, mean corpuscular hemoglobin concentration; MCV, mean corpuscular volume; MPV, mean platelet volume; PT, prothrombin time; RBC, red blood cells; WBC, white blood cells.

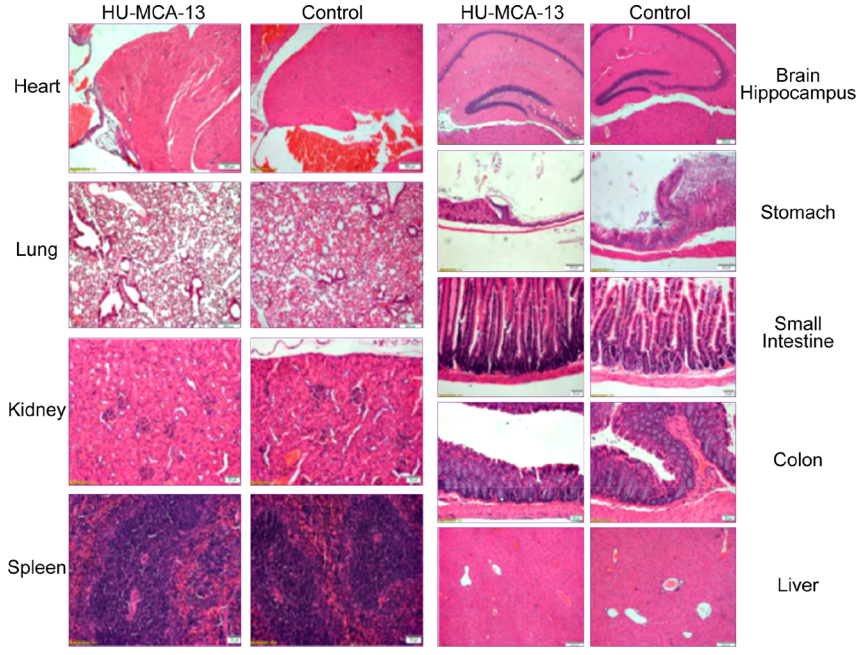


**Figure 5.** Representative histological images of organ slices stained with hematoxylin and eosin for acute toxicity test of male mice after oral administration of HU-MCA-13.

Table S1). The mortality and changes on body weight, clinical signs and gross observation, were monitored up to 30 days after treatment. We could not find any mortality at this high dose of 250 mg/kg. No significant changes on body weight were detected by comparing HU-MCA-13 250 mg/kg to 1% DMSO treated groups: they started with 21 and ended with 27 g body weight. The mice were examined for autonomic symptoms by measuring salivation, urinary delivery, pupillary constriction, hair contraction, etc., however, no differences were observed between the HU-MCA-13 and DMSO treated mice.

The hematopoietic system is one of the most sensitive parameters to assess the toxicity of drugs in humans and animals. Tail vein blood samples were taken from DMSO 1% treated control (n = 3) and 250 mg/kg HU-MCA-13-injected mice (n = 4) after 24 h from injection and submitted for


https://dx.doi.org/10.1021/acschemneuro.0c00255
ACS Chem. Neurosci. 2020, 11, 2577−2589

**Table 1. Screening in vitro of MCA-13 effects on selected GPCRs, ion channels, kinases, nuclear hormone receptors, enzymes and neurotransmitter transporters**

| Target Protein name | Target Gene name | Reference Compound[1] | Mode of action[2] | Functional Assay[3] | $RC_{50}(\mu M)$[4] | MCA-13 Max. Responce (%)[5] |
|---|---|---|---|---|---|---|
| **GPCRs** | | | | | | |
| Adenosine Receptor $A_{2A}$ | ADORA2A | NECA | Agonist | Calcium Flux | 0.01524 | 0 |
| | | SCH 442416 | Antagonist | | 0.04332 | 4.09 |
| Adrenergic Receptor $\alpha_{1A}$ | ADRA1A | A61603 | Agonist | Calcium Flux | 0.0011 | 1.12 |
| | | Tamsulosin | Antagonist | | 0.00096 | 3.06 |
| Adrenergic Receptor $\alpha_{2A}$ | ADRA2A | UK 14304 | Agonist | cAMP | 0.00066 | 24.55 |
| | | Yohimbine | Antagonist | | 0.02617 | 0 |
| Adrenergic Receptor $\beta_1$ | ADRB1 | Isoproterenol | Agonist | cAMP | 0.00125 | 1.92 |
| | | Betaxolol | Antagonist | | 0.02278 | 9.29 |
| Adrenergic Receptor $\beta_2$ | ADRB2 | Isoproterenol | Agonist | cAMP | 0.0016 | 1.29 |
| | | ICI 118,551 | Antagonist | | 0.00211 | 8.23 |
| Arginine Vasopressin Receptor $1_A$ | AVPR1A | $[Arg^8]$-Vasopressin | Agonist | Calcium Flux | 0.00052 | 0.29 |
| | | SR49059 | Antagonist | | 0.0029 | 0 |
| Cholecystokinin Receptor A | CCKAR | $(Tyr[SO_3H]_{27})$ Cholecystokinin Fragment 26–33 Amide | Agonist | Calcium Flux | 0.0002 | 1.56 |
| | | SR 27897 | Antagonist | | 0.0298 | 0 |
| Muscarinic acetylcholine Receptor $M_1$ | CHRM1 | Acetylcholine chloride | Agonist | Calcium Flux | 0.02359 | 0 |
| | | Atropine | Antagonist | | 0.00695 | 7.43 |
| Muscarinic acetylcholine Receptor $M_2$ | CHRM2 | Acetylcholine chloride | Agonist | cAMP | 0.02725 | 11.68 |
| | | Atropine | Antagonist | | 0.01538 | 0 |
| Muscarinic acetylcholine Receptor $M_3$ | CHRM3 | Acetylcholine chloride | Agonist | Calcium Flux | 0.04944 | 0.13 |
| | | Atropine | Antagonist | | 0.00612 | 8.81 |
| Cannabinoid Receptor 1 | CNR1 | CP 55940 | Agonist | cAMP | 0.00012 | 50.22 |
| | | AM251 | Antagonist | | 0.00466 | 0.57 |
| Cannabinoid Receptor 2 | CNR2 | CP55940 | Agonist | cAMP | 0.00033 | 49.59 |
| | | SR144528 | Antagonist | | 0.0491 | 4.11 |
| Dopamine Receptor $D_1$ | DRD1 | Dopamine | Agonist | cAMP | 0.17552 | 0 |
| | | SCH 39166 | Antagonist | | 0.0026 | 14.3 |
| Dopamine Receptor $D_2$ | DRD2S | Dopamine | Agonist | cAMP | 0.00321 | 0 |
| | | Risperidone | Antagonist | | 0.00589 | 0.51 |
| Endothelin Receptor Type A | EDNRA | Endothelin 1 | Agonist | Calcium Flux | 0.00036 | 0 |
| | | BMS 182874 | Antagonist | | 0.63689 | 0 |
| Histamine Receptor $H_1$ | HRH1 | Histamine | Agonist | Calcium Flux | 0.0155 | 0 |
| | | Mepyramine | Antagonist | | 0.01549 | 1.05 |
| Histamine Receptor $H_2$ | HRH2 | Histamine | Agonist | cAMP | 1.01395 | 1.78 |
| | | Tiotidine | Antagonist | | 0.06593 | 26.94 |
| 5-Hydroxy tryptamine (Serotonin) Receptor $1_A$ | HTR1A | Serotonin Hydrochloride | Agonist | cAMP | 0.01101 | 7.66 |
| | | Spiperone | Antagonist | | 0.08756 | 0 |
| 5-Hydroxy tryptamine (Serotonin) Receptor $1_B$ | HTR1B | Serotonin Hydrochloride | Agonist | cAMP | 0.0046 | 10.47 |
| | | SB 224289 | Antagonist | | 0.03853 | 0 |
| 5-Hydroxy tryptamine (Serotonin) Receptor $2_A$ | HTR2A | Serotonin Hydrochloride | Agonist | Calcium Flux | 0.0061 | 1.13 |
| | | Altanserin | Antagonist | | 0.01903 | 0 |
| 5-Hydroxy tryptamine (Serotonin) Receptor $2_B$ | HTR2B | Serotonin Hydrochloride | Agonist | Calcium Flux | 0.00263 | 0 |
| | | LY 272015 | Antagonist | | 0.00082 | 0.13 |
| Opioid Receptor Delta $_1$ | OPRD1 | DADLE | Agonist | cAMP | 0.00012 | 6.34 |
| | | Naltriben | Antagonist | | 0.00064 | 0 |
| Opioid Receptor Kappa $_1$ | OPRK1 | Dynorphin A (1–17) | Agonist | cAMP | 0.0481 | 7.89 |
| | | Nor- Binaltorphimine | Antagonist | | 0.0064 | 0 |
| Opioid Receptor Mu $_1$ | OPRM1 | DAMGO | Agonist | cAMP | 0.00194 | 9.31 |
| | | Naloxone | Antagonist | | 0.00552 | 0.38 |
| **Target Protein name** | **Target Gene name** | **Reference Compound[1]** | **Mode of action[2]** | **Functional Assay[3]** | **$RC_{50}(\mu M)$[4]** | **MCA-13 Max. Responce (%)[5]** |
| **Ion channels** | | | | | | |
| Voltage-gated L-type calcium channel | CAV1.2 | Isradipine | Blocker | Ion channel | 0.0225 | 3.82 |
| Gamma-aminobutyric acid Receptor A | GABAA | Picrotoxin | Blocker | | 5.91692 | 7.74 |
| | | GABA | Opener | | 8.51412 | 3.68 |
| Kv11.1, the alpha subunit of a potassium ion channel | hERG | Astemizole | Blocker | | 0.07136 | 0 |
| 5-Hydroxy-tryptamine (Serotonin) Receptor $3_A$ | HTR3A | Bemestetron | Blocker | | 0.00368 | 0.19 |



https://dx.doi.org/10.1021/acschemneuro.0c00255
ACS Chem. Neurosci. 2020, 11, 2577–2589

**Table 1. continued**

| Target Protein name | Target Gene name | Reference Compound[1] | Mode of action[2] | Functional Assay[3] | $RC_{50}(\mu M)$[4] | MCA-13 Max. Responce (%)[5] |
|---|---|---|---|---|---|---|
| | | Serotonin Hydrochloride | Opener | | 0.552217 | 0 |
| Kv7.1/KCNE Potassium voltage-gated channel | KvLQT1/ minK | XE 991 | Blocker | | 2.63679 | 0.55 |
| | | ML-277 | Opener | | 6.71743 | 0 |
| Nicotinic acetylcholine Receptor alpha-4 beta-2 | nAChR(a4/ b2) | Dihydro-AY-erythroidine | Blocker | | 0.70659 | 5.95 |
| | | Nicotine | Opener | | 2.18712 | 0 |
| A tetrodotoxin-resistant voltage-gated sodium channel | NAVI1.5 | Lidocaine | Blocker | | 41.01752 | 0 |
| *N*-methyl-D-aspartate (NMDA) Glutamate Receptor $1_A/2_B$ | NMDAR (1A/2B) | MK 801 | Blocker | | 0.05277 | 0 |
| | | L-Glutamic Acid | Opener | | 0.96247 | 0 |
| **Kinases** | | | | | | |
| Insulin Receptor (tyrosine kinase) | INSR | BMS-754807 | Inhibitor | Binding | 0.0009 | 3.22 |
| Lymphocyte Cell-Specific Protein-Tyrosine Kinase (Src family) | LCK | Gleevec | Inhibitor | | 0.07191 | 12.77 |
| Rho Associated Coiled-Coil Containing Protein Kinase 1 (serine-threonine kinase) | ROCK1 | Staurosporine | Inhibitor | | 0.00034 | 21.61 |
| Vascular endothelial growth factor receptor 2 (KDR tyrosine kinase) | VEGFR2 | SU-11248 | Inhibitor | | 0.00033 | 21.68 |
| **Nuclear Hormone Receptors** | | | | | | |
| Nuclear Hormone Androgen Receptor | AR | 6a-Fluorotestosterone | Agonist | Nuclear Hormone Receptor | 0.00646 | 0 |
| | | Geldanamycin | Antagonist | | 0.08646 | 5.27 |
| Nuclear Hormone Glucocorticoid Receptor | GR | Dexamethasone | Agonist | | 0.10198 | 0 |
| | | Mifepristone | Antagonist | | 0.10906 | 2.28 |
| **Enzymes** | | | | | | |
| Acetylcholinesterase | AChE | Physostigmine | Inhibitor | Enzymatic | 0.0282 | 4.27 |
| Cyclooxygenase 1 | COX 1 | Indomethacin | Inhibitor | | 0.06281 | 24.99 |
| Cyclooxygenase 2 | COX 2 | NS −398 | Inhibitor | | 0.07376 | 7.99 |
| Monoamine oxidase type A | MAOA | Clorgyline | Inhibitor | | 0.00217 | 1.86 |
| cGMP-inhibited cyclic nucleotide phospho-diesterase 3A | PDE3A | Cilostamide | Inhibitor | | 0.02113 | 3.21 |
| cAMP-specific 3′,5′-cyclic phospho-diesterase 4D2 | PDE4D2 | Cilomilast | Inhibitor | | 0.01549 | 0 |
| **Catecholamine Transporters** | | | | | | |
| Dopamine transporter | DAT | GBR 12909 | Blocker | Transporter | 0.0076 | 0 |
| Norepinephrine transporter | NET | Desipramine | Blocker | | 0.01089 | 3.53 |
| Serotonin transporter | SERT | Clomipramine | Blocker | | 0.00878 | 15.45 |

[1]Full chemical names of reference compounds: *NECA,* 5′-(N-Ethylcarboxamido)adenosine; *SCH 442416,* 2-(2-furyl)-7-[3-(4-methoxyphenyl)-propyl]-7H-pyrazolo[4,3-*e*][1,2,4]triazolo[1,5-*c*]pyrimidin-5-amine;*A61603,* N-(5-(4,5-Dihydro-1H-imidazol-2-yl)-2-hydroxy-5,6,7,8-tetrahydro-naphthalen-1-yl)methanesulfonamide hydrobromide; *Tamsulosin,* 5-(2-((2-Ethoxyphenoxy)ethyl)amino) propyl −2-methoxybenzenesulfonamide; *UK 14304,* 5-Bromo-N-(2-imidazolin-2-yl)-6-quinoxalinamine; *Yohimbine,* methyl (1S,15R,18S,19R,20S)-18-hydroxy1,3,11,12,14,15, 16,17,18,19,20,21- dodecahydroyohimban-19-carboxylate; *Isoproterenol,* 4-[1-hydroxy-2-(propan-2-ylamino)ethyl]benzene-1,2-diol;*Betaxolol,* 1-[4-[2-(cyclopropylmethoxy)ethyl ]phenoxy]-3-(propan-2-ylamino)propan-2-ol; *Isoproterenol,* 4-[1-hydroxy-2-(propan-2-ylamino)ethyl]benzene-1,2-diol; *ICI 118551,* (2*R*,3*S*)-1-[(7-methyl-2,3-dihydro-1H-inden-4-yl)oxy]-3-(propan-2-ylamino)butan-2-ol;hydrochloride; *SR49059,* (2S)-1-[[(2*R*,3*S*)-5-Chloro-3-(2-chlorophenyl)-1-[(3,4-dimethoxyphenyl)sulfonyl]-2,3-dihydro-3-hydroxy-1H-indol-2-yl]carbonyl]-2-pyrrolidinecarboxamide; *SR 27897,* 2-[[[4-(2-chlorophenyl)-2-thiazolyl]amino]carbonyl]-1H-indole-1-acetic acid; *CP 55940,* 5-(1,1-Dimethylheptyl)-2-[5-hydroxy-2-(3-hydroxypropyl)cyclohexyl]phenol; *CP55940,* 5-(1,1-Dimethylheptyl)-2-[5-hydroxy-2-(3-hydroxypropyl)cyclohexyl]phenol; *AM251,* 1-(2,4-Dichlorophenyl)-5-(4-iodophenyl)-4-methyl-N-1-piperidinyl-1H-pyrazole-3-carboxamide; *SR144528,* 5-(4-Chloro-3-methylphenyl)-1-[(4-methylphenyl)methyl]-N-[(1S,2S,4R)-1,3,3-trimethylbicyclo[2.2.1]hept-2-yl]-1H-pyrazole-3-carboxamide; *SCH 39166,* (6aS-trans)-11-Chloro-6,6a,7,8,9,13b-hexahydro-7-methyl-5H-benzo[d]naphth[2,1-*b*]azepin-12-ol hydrobromide; *BMS 182874,* 5-(Dimethylamino)-N-(3,4-dimethyl-5-isoxazolyl)-1-naphthalenesulfonamide hydrochloride; *SB 224289,* 1′-Methyl-5-[[2′-methyl-4′-(5-methyl-1,2,4-oxadiazol-3-yl)biphenyl-4-yl]-carbonyl]-2,3,6,7-tetrahydrospiro[furo[2,3-*f*]indole-3,4′-piperidine hydrochloride; *LY 272015,* 1-[(3,4-Dimethoxyphenyl)methy]-2,3,4,9-tetrahydro-6-methyl-1H-pyrido[3,4-*b*]indole hydrochloride; *XE 991,* 10,10-bis(4-pyridinylmethyl)-9(10H)-anthracenone; *ML-277,* (2R)-N-[4-(4-Methoxyphenyl)-2-thiazolyl]-1-[(4-methylphenyl)sulfonyl]-2-piperidinecarboxamide; *MK 801,* (2R)-N-[4-(4-Methoxyphenyl)-2-thiazolyl]-1-[(4-methylphenyl)sulfonyl]-2-piperidinecarboxamide; *BMS-754807,* (2S)-1-[4-[(5-cyclopropyl-1H-pyrazol-3-yl)amino]pyrrolo[2,1-*f*][1,2,4]triazin-2-yl]-N-(6-fluoropyridin-3-yl)-2-methylpyrrolidine-2-carboxamide; *SU-11248,* N-[2-(Diethylamino)ethyl]-5-[(Z)-(5-fluoro-1,2-dihydro-2-oxo-3H-indol-3-ylidene)methyl]-2,4-dimethyl-1H-pyrrole-3-carboxamide (2S)-2-hydroxybutanedioic acid; *NS −398,* 4-[5-(4-methylphenyl)-3-(trifluoromethyl)pyrazol-1-yl]benzenesulfonamide; *GBR 12909,* 1-(2-[bis(4-Fluorophenyl)methoxy]ethyl)-4-(3-phenylpropyl)piperazine dihydrochloride. [2]The mode of interaction with the biological target. [3]The assay describing the major function of the biological target. [4]Reference compound effective concentration 50%. [5]**HU**-MCA- 13 maximal response (activation or inhibition) at a concentration of 10 $\mu$M.

hematocrit cell counting and biochemical analysis. Blood analyses are depicted in Figure 4. No difference in blood count (Figure 4A), electrolytes (Figure 4B) and coagulation parameters (Figure 4C) was noted between the DMSO and



https://dx.doi.org/10.1021/acschemneuro.0c00255
ACS Chem. Neurosci. 2020, 11, 2577−2589

HU-MCA-13-injected mice. The coagulation biomarkers (international normalized ratio, prothrombin time, activated partial thromboplastin time, fibrinogen) were not affected by the exposure to HU-MCA-13 (Figure 4C) and similar to control mice.[28] Of special importance are normal liver (ALP, alkaline phosphatase; ALT, alanine transaminase and AST, aspartate transaminase) functions and normal kidney (creatinine and blood urea nitrogen) functions, indicating sufficient organ integrity at the end of the experimental period. The data obtained was similar to hematological parameters reported for this mice strain[29] and clearly indicates lack of differences on kidney and liver parameters (Figure 4D) between the two mice groups. There was a small significant increase in HU-MCA-13-injected mice on bilirubin concentration, a finding deserving further investigation. Cumulatively these blood analyses indicate acute tolerability of 250 mg/kg HU-MCA-13 upon IV injection in C57BL/6 male mice.

Prioritizing compounds with a lower chance of causing toxicity, early in the drug discovery process, would help in the drug development process.[30] With this consideration we conducted acute (single-dose) toxicity study[31] to determine the short-term adverse pathological effects on major mice organs of HU-MCA-13 when administered in mice in a single dose, for a period of 24 h. One group of 5 mice received HU-MCA-13 orally at a dose of 2000 mg/kg, dissolved in a nano-emulsifying drug delivery system[32] in a bolus of 0.4 mL/mouse. After 24 h exposure, the animals were sacrificed, and organs were harvest for pathology analyses. In general, in all organs no cytotoxic lesions were found (Figure 5). In three animals administered with HU-MCA-13, we found in the last part of the colon, rectum and the adjacent anal unhaired skin a severe purulent, necrotizing inflammation. This finding was not related to the tested compound and was considered as an accidental finding. This information on the lack of acute toxicity of HU-MCA-13 may predict the safety of this compound in future therapeutic evaluation.

*HU-MCA-13 safety by in vitro pharmacological profiling.* "Off-target" activity refers to all other targets for which a molecule has affinity with the outcome of activation, blockade, or modulation, resulting in a functional effect. In many cases, the off-target activity of the molecule can be sub-clinical and not pose a concern. On the other hand, the off-target activity may result in side effects of the active agent that range from a minor nuisance to a severe adverse event, resulting with drug withdrawal.[33] Therefore, in vitro pharmacological profiling is increasingly being used earlier in the drug discovery process to identify undesirable off-target activity profiles that could hinder or halt the development of a candidate drug.[34] With this background, assessing the specificity of HU-MCA-13 early in its development using highly relevant and predictive functional assays, which allow more informed decisions about its safety, ultimately lead to the development of an effective neurotropic drug. Tacking in account these considerations, we performed different pharmacological assays using DiscoverX's SAFETY-scan, accumulating data points regarding the potential functional interaction (activation, inhibition, lack of effect) of HU-MCA-13 with physiological targets that includes G protein-coupled receptors (GPCRs), ion channels, transporters, nuclear hormone receptors, and some enzymes (Supporting Information, Figures Sup. 1 and 2), targets known to show a clear correlation with observed in vivo toxic effects.[34] We choose to investigate a concentration of 10 $\mu$M HU-MCA-13 which was not toxic to neurons and found very active in stimulating neurite outgrowth. We set a threshold of 25% for inhibition or potentiation of activity on all tested targets as summarized in Table 1. The maximal response upon treatment with 10 $\mu$M HU-MCA-13 indicated that this compound was not interacting with the majority of the targets, with the exception of the following G-protein coupled receptors (GPCRs): agonistic activity (increased cAMP level) toward $\alpha$2A-adrenergic receptor ADRA2A (24.5%); Cannabinoid receptor $CB_1$−CNR1 (50.1%) Cannabinoid receptor CB2-CNR2 (49.6%) and antagonistic activity (inhibition of cAMP level by 26.9%) toward Histamine H2 receptor HRH2. Moreover, HU-MCA-13 inhibited by 25% Cyclooxygenase-1 activity (Table 1). These findings may predict that these GPCRs and COX-1 may represent potential molecular targets of MCA-13, and that upon using toxic, overdoses of HU-MCA-13 in animal or human studies, physiological effects will be observed on blood pressure, adrenaline release, sedation, increase of GI motility and insulin secretion (ADRA2 related), euphoria and dysphoria, anxiety, memory impairment and poor concentration, analgesia, hypothermia, increase in weight loss, emesis, depression (CNR1 related), increased inflammation and reduction of bone mass (CNR2 related) and effects on gastric acid secretion, emesis, positive heart inotropic effects (HRH2 related) as well as gastric and pulmonary bleeding, dyspepsia and renal dysfunction (COX-1 related).[34]

"On-target" activity refers to the site of action of the test substance (e.g., target receptor or enzyme) that results in the desired pharmacodynamic effect associated with the treatment of disease.[35] Since the mechanism of HU-MCA-13 induced neurotropic effect is unknown, present findings may also suggest the involvement of ADRA2A, CB1-CNR1 and/or CB2-CNR2, HRH2 and COX-1 in HU-MCA-13-induced neurite outgrowth. This hypothesis is based on the reports indicating that activation of ADRA2A[36] and CB1-CNR1[37] in PC12 cell cultures and inhibition of COX-1 in cholinergic neuroblastoma NG108-15 cells[38] triggered neurite outgrowth.

Prostaglandin $E_2$ ($PGE_2$) is one of the major lipid mediators produced by the arachidonic acid cascade. Arachidonic acid is produced in neurons by phospholipases $A_2$ family members and is converted to $PGE_2$ by cyclooxygenase (COX)-1 and -2. It was reported that NGF induced COX-1 expression and enzymatic activity in PC12 cells.[39] $PGE_2$ can enhance neuronal differentiation expressed by stimulation of neurite outgrowth in neuroblastoma cell lines such as mouse NG108-15 cells[40] and mouse DRG neurons.[41] Therefore, to evaluate the possibility that HU-MCA-13 affects the $PGE_2$ production in PC12 cells, we treated the cultures for 24 h with either different concentrations of HU-MCA-13 or 1 $\mu$g/mL LPS, the lipopolysaccharide bacterial product known to increase $PGE_2$ production, cultures' media was collected and $PGE_2$ was measured by ELISA (Figure 6A). It is evident that HU-MCA-13 increased $PGE_2$ production in a dose-dependent fashion by 3−6-fold over that produced by control, untreated cultures. In another experiment, we investigated the individual and combined effect of 50 ng/mL NGF and 1 $\mu$M HU-MCA-13 on production of $PGE_2$ after 24 h treatment of the PC12 cell cultures (Figure 6B).[42] NGF significantly increased the production of $PGE_2$ but the combined effect with HU-MCA-13 was weekly additive. These findings further support the involvement of $PGE_2$ production in HU-MCA-13 induced neurotropic effect and are calling for additional research to clarify how partial inhibition of COX-1 affects arachidonate


https://dx.doi.org/10.1021/acschemneuro.0c00255
ACS Chem. Neurosci. 2020, 11, 2577−2589

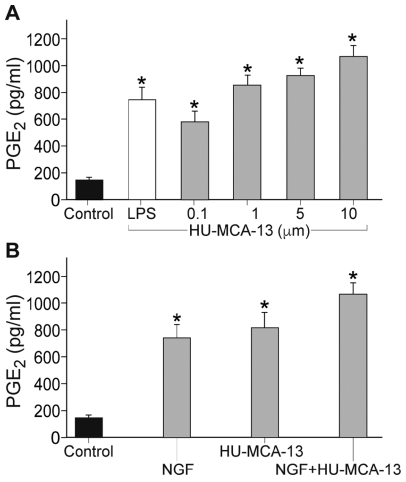


**Figure 6. HU-MCA-13 induced release of $PGE_2$in PC12 cells.** A. Dose response. The cultures were treated with either 1 $\mu$g/mL LPS or different concentrations of HU-MCA-13 for 24 h. B. The combined effect of 50 ng/mL NGF and 1 $\mu$M HU-MCA-13 on production of $PGE_2$ after 24 h treatment. The media was collected and $PGE_2$ was measured by ELISA. Values are mean ± SD ($n$ = 6); *$p$ < 0.01 compared to control.

metabolic pathway in relation to MCA-13 induced neurotropic activity.

*HU-MCA-13 safety by in vitro evaluation using PhosphoSens CSox based kinase assays.* The initial focus was to measure the modulatory activity in vitro of MCA-13 on protein kinases which were reported to be involved in induction of neurite outgrowth.[18,43] To do this, we took advantage of a powerful method to measure the activity of recombinant protein kinases using a homogeneous and continuous (kinetic) format, where the level of chelation-enhanced fluorescence (CHEF) is directly proportional to the amount of phosphorylated, real-time sensors consisting of sulfonamido-oxine (Sox) chromophore linked to a peptide or protein substrates of selective kinases.[44] This assay is ideal for elucidating drug mechanism of action and is increasingly being applied earlier in the drug development workflow to address off target effects and/or the challenges and opportunities for next generation protein kinase inhibitors.[45] Since neurotrophins induce neurite outgrowth by activating the different tropomyosin kinase receptors (Trk), and small molecules agonists of Trk receptors can selectively activate Trks,[46] we first investigated the ability of HU-MCA-13 to modulate TRKA, TRKB and TRKC phosphorylation activities (Supporting Information, Figure S3-2). We found no effects of HU-MCA-13 on TRKA and TRK B and a a slight inhibitory effect on TRKC (no effect on the initial rate, so not inhibition, but rather a small delay in the later stage of the progress curve as it approaches the maximum signal (RFU Max), which can reflect reduced stability of the kinase). The TRKs constructs used in the assay contained only the intracellular kinase domain (amino acids 442−786) and therefore presently we cannot exclude that HU-MCA-13 may interact with the TRKs extracellular domain thereby inducing the conformational change required for the kinase domain activation. However, this possibility is less likely, considering that K252a Trk A inhibitor did not abolished HU-MCA-13 neurotropic effect (Figure 3A). Moreover, no effects of HU-MCA-13were found on other kinases (ASK1, ERK2, JNK3, p38$\alpha$, CDK5, KDR-VEGFR, AKT1, GSK3$\beta$, PDGFR$\beta$, PKAC$\alpha$, PKC, CK1, IKK$\beta$) which stimulate neurite outgrowth. Also, no effects were observed of HU-MCA-13 on kinases (EGFR, IGF1R, FGFR 1 and 2, CAMK2$\alpha$,) which inhibit neurite outgrowth or calcineurin phosphatase which dephosphorylates the neurite outgrowth stimulatory protein, cofilin.[47] The inability of 5 $\mu$M HU-MCA-13 to inhibit/activate significantly any of the kinases or phosphatase tested further confirm the kinases data from DiscoverX's SAFETYscan and indicate off target safety of HU-MCA-13.

Although, the cellular signaling direct mechanisms responsible for the neurotropic action of HU-MCA-13 compounds were not directly addressed in the present research, we would like to propose a few hypotheses. In view of the strong neurotropic effect of HU-MCA-13 in the different neuronal systems investigated (Figures 1−3), the first option to be considered is that this compound activates directly the TrkA-NGF receptor, representing an agonist inducing receptor tyrosine kinase activation, which in turn phosphorylates cytoskeletal and other neuronal substrates to induce the neurotropic effect. This possibility is less likely, considering the inability of K252a-TrkA inhibitor to block HU-MCA-13 neurotropic effect (Figure 3) and the lack of HU-MCA-13 stimulatory effects on Trk receptors as evaluated by in vitro phosphorylation using PhosphoSens CSox based kinase assays (Supporting Information). Alternatively, present findings may also suggest the involvement of ADRA2A, CB1-CNR1 and/or CB2-CNR2, HRH2 and COX-1 (Table 1) in HU-MCA-13-induced neurite outgrowth. The third hypothesis considers that HU-MCA-13 compound affects the cytoskeleton of the PC12 cells, either by interacting with the microtubules or tau proteins as evident from $\beta$ tubulin III immunostaining (Figure 2), and therefore, inducing the neurotropic activity. Based on the finding that HU-MCA-13 increased PGE2 levels (Figure 6), the fourth most plausible hypothesis suggests that prostaglandin PGE2 and/or other arachidonic acid metabolite contribute to HU-MCA-13 neurotropic effect. While other mechanisms can still be addressed for a comprehensive understanding of HU-MCA-13-induced neurotropic effect, current findings may provide starting clues to the molecular mechanisms of HU-MCA-13-induced neurotropic effect. Future molecular, pharmacokinetic and pharmacodynamic research is required to optimize HU-MCA-13 as a new drug candidate for polyneuropathy therapy.

In summary, present findings indicate that HU-MCA-13 analogue (3-(3-allyl-2 methylenecyclohexyl) propanoic acid is a promising neurotropic, safe, lead compound for further drug development toward polyneuropathy therapy.

## 3. MATERIALS AND METHODS

**Neurotropic activity and safety.** DMEM media, fetal calf (FCS) and horse (HS) serums, penicillin and streptomycin were purchased from Biological Industries (Beit Haemek, Afula, Israel). Type IV collagenase and DMSO was purchased from Sigma-Aldrich Merck, St Louis, MO, USA. Tissue culture grade mouse $\beta$-NGF, was purchased from Alomone Laboratories (Jerusalem, Israel). The mouse anti-neuron-specific $\beta$III-tubulin (clone TuJ-1) monoclonal antibody (catalog number: MAB1195) and the $PGE_2$-specific, ELISA kit (Catalogue number KGE004B) were purchased from R&D Systems Inc. Minneapolis, MN, USA. Cy3-conjugated goat anti-mouse antibody was purchased from Jackson ImmunoResearch Labs, West Grove, PA, USA.

**Synthesis.** Unless otherwise stated, all reagents were purchased from commercial suppliers and used without further purification. Reactions were monitored by thin-layer chromatography (TLC) on


https://dx.doi.org/10.1021/acschemneuro.0c00255
ACS Chem. Neurosci. 2020, 11, 2577−2589

silica gel 60-$F_{254}$ aluminum plates (Merck) and/or gas chromatography−mass spectrometry (GCMS). Visualization of compounds on TLC was accomplished by irradiation with UV light at 254 nm and/or vanillin stain. GCMS Analysis was performed with Agilent 7820A gas chromatograph equipped with Agilent 5975 quadrupole mass selective detector, using Agilent HP-5MS capillary column (30 m, 0.25 mm, 0.25 $\mu$m film). Column chromatography was performed using silica gel 60 (particle size 0.040−0.063 mm) purchased from Sigma-Aldrich. Proton and carbon NMR spectra were recorded on Varian Mercury 300 MHz spectrometer in deuterated solvent. Proton chemical shifts are reported in ppm ($\delta$) relative to tetramethylsilane with the solvent resonance employed as the internal standard ($CDCl_3$, $\delta$ 7.26 ppm). $^{13}C$ Chemical shifts are reported in ppm from tetramethylsilane with the solvent resonance as the internal standard ($CDCl_3$, $\delta$ 77.0 ppm). Data is reported as follows: chemical shift, multiplicity (*s* = singlet, *d* = doublet, *t* = triplet, *q* = quartet, *m* = multiplet), integration and coupling constants (Hz). High resolution mass spectra were determined on a ThermoScientific LTQ Orbitrap XL (FTMS). Infrared (IR) spectra were recorded on a ThermoFischer Scientific NICOLET iS10 spectrometer.

All compounds were prepared according to the general procedures reported in ref21, 24.

*3-(3-allyl-2-oxocyclohexyl)propanenitrile (2).* 1-(cyclohex-1-en-1-yl)pyrrolidine was prepared by refluxing cyclohexanone (35.2 mmol, 3.45 g, 1.0 equiv) and pyrrolidine (105.6 mmol, 8.63 mL, 3.0 equiv) in dry toluene (35.0 mL,1 M), in the presence of catalytic amount of *p*TSA, until all water was distilled by Dean−Stark apparatus. After removal of toluene and traces of pyrrolidine by vacuum evaporation, to the crude compound was added dry $CH_3CN$ (35.0 mL) followed by dropwise addition of Acrylonitrile (1.0 equiv., 35.2 mmol, 2.3 mL) and the mixture was stirred for 3 h at 40 °C. DIEA (1.0 equiv, 35.2 mmol, 6.1 mL) was added as one portion, followed by slow addition of allyl bromide (1.0 equiv., 35.2 mmol, 3.0 mL). The mixture was stirred for 12 h at 80 °C, then quenched with water and refluxed for 1 h. Purification of the crude product by flash column chromatography (10% ethyl acetate in hexane) yielded pure 3-(3-allyl-2-oxocyclohexyl)propanenitrile (2.24 g, 35% yield, light orange oil). $^1H$ NMR (300 MHz, $CDCl_3$): $\delta$ 5.82−5.68 (m, 1H), 5.04−4.97 (m, 2H), 2.55−2.33 (m, 5H), 2.22−1.68 (m, 6H), 1.56−1.21 (m, 3H). $^{13}C$ NMR (75 MHz, $CDCl_3$): $\delta$ 212.0, 136.2, 136.2, 116.3, 50.5, 49.1, 35.2, 34.6, 33.4, 25.4, 25.1, 15.2. IR (neat): 2933, 2245, 1706, 1640, 1447, 912 $cm^{-1}$. HRMS (*m*/*z*) calcd for $C_{12}H_{17}NONa$ ($[M + Na]^+$): 214.1202; found: 214.1203.

*3-(3-Allyl-2-methylenecyclohexyl)propanenitrile (3).* Methyltriphenylphosphonium bromide (24.3 mmol, 8.7 g) and potassium *tert*-butoxide (24.3 mmol, 2.7 g) were stirred at 40 °C in dry THF (0.4 M) for 2 h. A 3 M solution of 3-(3-allyl-2-oxocyclohexyl)-propanenitrile (12.2 mmol, 2.3 g) in dry THF was added dropwise at 0 °C and the mixture was stirred for 2 h at room temperature. Water was added, and the aqueous layer was extracted twice with diethyl ether. The combined organic layers were dried ($Na_2SO_4$), filtered, and the solvent was removed under reduced pressure. Purification of the residue by flash column chromatography (10% ethyl acetate in hexane) yielded pure 3-(3-allyl-2-methylenecyclohexyl)propanenitrile as a mixture of diastereoisomers (1.9 g, 86% yield, yellow oil). $^1H$ NMR (300 MHz, $CDCl_3$): $\delta$ 5.87−5.73 (m, 1H), 5.06−4.99 (m, 2H), 4.74−4.58 (m, 2H), 2.44−2.32 (m, 3H), 2.07−1.42 (m, 9H), 1.10−0.87 (m, 2H). $^{13}C$ NMR (75 MHz, $CDCl_3$): major diastereoisomer: $\delta$ 154.3, 137.5, 137.4, 115.8, 107.6, 102.6, 43.8, 43.1, 37.5, 34.9, 28.2, 25.7, 15.2; minor diastereoisomer, characteristic signals: $\delta$ 152.1, 120.0, 41.9, 39.7, 36.7, 33.4, 33.1, 27.5, 21.3, 15.3. IR (neat): 2923, 2245, 1640, 1444, 1392, 1333, 994, 891 $cm^{-1}$. HRMS (*m*/*z*) calcd. for $C_{13}H_{19}NNa$ ($[M + Na]^+$): 212.14097; found: 212.14099.

*3-(3-allyl-2-methylenecyclohexyl)propanoic acid (MCA-13).* A mixture of 3-(3-allyl-2- methylenecyclohexyl)propanenitrile (1.0 equiv., 10.6 mmol, 2.0 g), ethanol (70 mL) and 65% aq. NaOH (212.0 mmol, 8.5 g) was stirred at 80 °C for 3 h. The mixture was concentrated under vacuum and the residue was quenched with water. The aqueous solution was extracted with ether, acidified with conc. HCl to pH = 1 and then extracted again with ethyl acetate. The mixture was dried over $Na_2SO_4$, filtered and evaporated to yield 3-(3-allyl-2-methylenecyclohexyl)propanoic acid as mixture of diastereoisomers (2.2 g, 98% yield, orange oil). $^1H$ NMR (300 MHz, $CDCl_3$): $\delta$ 11.35 (bs, 1H), 5.88−5.75 (m, 1H), 5.07−4.98 (m, 2H), 4.70−4.66 (m, 2H), 2.46−2.29 (m, 3H), 2.07−1.39 (m, 9H), 1.20−0.89 (m, 2H). $^{13}C$ NMR (75 MHz, $CDCl_3$): major diastereoisomer: $\delta$ 180.8, 155.1, 137.7, 115.6, 102.3, 43.9, 43.6, 37.2, 35.3, 35.0, 32.1, 27.3, 25.9; minor diastereoisomer, characteristic signals: $\delta$ 153.4, 137.5, 115.5, 106.6, 42.2, 39.8, 36.8, 33.5, 33.4, 32.3, 26.7, 21.3. IR (neat): 2924, 1705, 1640, 1414, 1280, 890 $cm^{-1}$.

**PC12 cells.** PC12 cells were cultured in T-200 flasks in high glucose (4.5 gr/L) DMEM medium supplemented with 7% FCS, 7% horse serum and 1% penicillin and streptomycin. Cells will be maintained at 37 °C in a humidified incubator containing 6% $CO_2$. All experiments were carried out in a GMP grade C clean room, according to ISO 7 requirements (10,000 particles/$m^3$). For neurotropic experiments, tissue culture Falcon plates were coated with 200 $\mu$g/mL collagen type 1 and placed under UV light for 30 min for sterilization. Thereafter, one ml of PC12 cell suspension (5000 cells/well) was applied in 12 or 24 well plate, respectively. The cultures were maintained in the incubator 2 days before exposure to investigated compound. Each neurotropic experiment contained two controls. The first consisted of untreated cells (negative control), representing the random effect: "noise signal", the ability of cells to spontaneously express neurite outgrowths which in 7 days are of a length less than 2-fold cell diameter. Also, negative controls consisted of cultures treated with 1% DMSO, solvent used to solubilize MCA-13. The positive controls represented neuronal cultures treated with 50 ng/mL NGF, indicating maximal neurite outgrowth that can be achieved in this model. The experimental group consisted of PC12 cells treated with different concentrations of MCA-13 or NGF and their combinations. In each experiment, after two and 7 days, six cultures were evaluated for neurotropic effect. These consecutive observations allow measurement of the progress of neurite outgrowth elongation and the percentage of cells with neurites.[48] In order to assess neurotropic effect, the neurite outgrowth length in each culture was quantified. For this purpose, each culture was placed under an inverted microscope and photographed by the attached camera. Each well was photographed at three to five representative areas. After acquiring the photos, they were analyzed by ImageJ, NIH software. The neurite outgrowth was estimated by fractal dimension ($D_f$), a statistical parameter that describes the fractional space (area and length) filled by neurite outgrowth.[21] $D_f$ ranged from 0 to 1.20. This method estimated the number of pixels covered by neurites/cells compared to empty space per square field, and therefore plotting log (number of square boxes) vs log (size in pixels) relationship generated a linear curve with $D_f$ representing the slope of the curve. Every photograph that was taken, was opened in a Photoshop software and a new layer was generated on it. Using a 5-pixel wide digital pencil tool, all the outgrowths were marked and the layer with the markers (outgrowth network) were saved in a 0−255 gray scale. Thereafter, the saved layer was opened by ImageJ NIH software. The software was "skeletonised" the layer, measuring the length and complexity of every outgrowth in a fractal box count and calculated the fractional dimension parameter ($D_f$).[49]

**DRG neurons.** To perform these experiments, 10 DRGs were excised under sterile conditions and transferred to Dulbecco's Modified Eagle Medium (DMEM) containing 0.25% Type IV collagenase in at 37 °C for 45 min, followed by a 20 min incubation with 0.025% trypsin in DMEM, to digest the associated connective tissue surrounding the neurons. After plating the ganglia onto collagen (50 $\mu$g/mL)/laminin mixture (5 $\mu$g/mL)-coated tissue culture wells for 24 h, DRG neurons were cultured for additional 1−7 days in fresh Neurobasal A/B27 medium[27] containing either 50 ng/mL NGF (positive control), medium containing 1% DMSO (negative control) or 5 $\mu$M MCA-13. The living cultures were photographed and thereafter, the ganglia were immunostained for $\beta$ tubulin III and again photographed using a fluorescent microscope. A researcher blinded to the experimental conditions performed image analysis, and the neurite outgrowth length (in micrometers) was measured.[50]


https://dx.doi.org/10.1021/acschemneuro.0c00255
ACS Chem. Neurosci. 2020, 11, 2577−2589

**Spinal cord neurons.** Spinal cords were isolated from adult rats (4−6 months old), and the meninges were removed from the spinal cord. The spinal cord was then cut into small pieces and collected in cold Hibernate A (Brainbits, Springfield, IL, USA), glutamine (0.5 mM), and B27 (Invitrogen, Carlsbad, CA). Briefly, dissected pieces of adult rat spinal cord tissue were maintained in phosphate-buffered saline (PBS) without $Ca^{2+}$ and $Mg^{2+}$ and pooled together and transferred to an enzymatic dissociation media containing 20 IU/ml papain in Earle's balanced salt solution (Worthington Biochemical, Freehold, NJ) and incubated for 30 min at 37 °C. After enzymatic dissociation, the papain solution was aspirated and the tissue was mechanically triturated with a fire-polished Pasteur pipet in 6 mL of complete media of fresh Hibernate A, glutamine (0.5 mM), and B27 containing 2000 IU/ml DNase and 10-mg/mL protease inhibitors. Thereafter, the cell suspension was layered over a 4 mL step gradient (Optipep diluted 0.505:0.495 [v/v] with Hibernate A−glutamine 0.5 mM−B27) and then made to 15, 20, 25, and 35% (v/v) in Hibernate A−glutamine 0.5 mM−B27 followed by centrifugation for 15 min, using 800 g, at 4 °C. The top 7 mL of the supernatant was aspirated. The next 2.75 mL from the major band was collected and diluted in 5 mL Hibernate A−B27 and centrifuged at 600 × g for 2 min. The pellet was suspended in Hibernate A−B27 and, after a second centrifugation, was suspended in the culture medium. The cell suspensions was plated on pre-coated collagen IV/laminin mixture-coated 96-well plates (Becton-Dickinson, Bedford, MA) at a density of $1.0 \times 10^4$ cells/well.[51] The spinal cord neurons were maintained for 1 day in culture and then treated with 1% DMSO−DMEM or 10 μM MCA-13 for 7 days. The cultures were photographed, and Image analysis was performed. Neurite outgrowth was measured and presented as mean length of a neurite (microns). To measure neuronal survival, 450 cells were counted in 10 randomly chosen microscope fields of a known area in each of the three dishes per condition using a 20× objective and phase-contrast optics. Counts of adherent cells were carried out 3 h after plating, and counts of neurite outgrowth-bearing cells were carried out on cells at 48 h. Cell survival was estimated by expressing the density of neurite outgrowth-bearing cells at 48 h as a percentage of the density of adherent cells at 3 h. This method reduced the possibility that counts included non-neuronal cells, which do not elaborate extensive neurite outgrowths but might result in a failure to count some neurons at 48 h if those cells failed to extend neurite outgrowths at this time point.

**Indirect immunofluorescence microscopy.** All neuronal cells cultures were grown on glass coverslips at 37 °C and 5% $CO_2$. Cells were then washed twice with PBS, fixed for 15 min with 3.7% paraformaldehyde at room temperature, and permeabilized for 1 min with 0.5% Triton X-100 in PBS on ice. Cells were then incubated for 3 h at room temperature with 15 μg/mL anti-neuron-specific βIII-tubulin mouse $IgG_{2A}$ (Clone # TuJ-1) monoclonal antibody diluted in PBS containing 10% normal goat serum. Cells were rinsed in PBS and labeled with Cy3-conjugated goat anti-mouse antibody (1:100) for 2 h at room temperature. Cells were then rinsed with PBS. Coverslips were mounted on glass slides. All images were collected with an Olympus FV1000 confocal scanner mounted on an IX-81 microscope using an UPlanApo 60×, NA 1.42 lens.

**Cytotoxicity.** Cell death was evaluated by morphological appearance of the cells and release of LDH into the medium, in the absence and presence of different concentrations of synthetic compounds as previously described.[52]

**$PGE_2$ measurements.** Aliquots of the culture media of PC12 cells treated for 48 h with either 1 μ g/mL LPS, 50 ng/mL NGF or 5 μM MCA-13 were assayed for $PGE_2$ using an $PGE_2$ -specific, ELISA kit, according to the manufacturer's instructions. The amount of $PGE_2$ in pg/mL was calculated from a $PGE_2$ standard curve, with a sensitivity of 41.4 pg/mL. Values are mean ± SD (n = 4) Statistical differences between groups were determined by Student' s *t* test and ANOVA followed by Bonferroni post-test and were considered significant when $^*p < 0.01$ compared to control.

**Pathological Analysis of Major Organs.** C57Bl/6 mice, 8 weeks old, obtained from Envigo animal breeding center were used in the study. All experiments were approved by the Institutional Animal Care and Use Committee and performed according to OECD guidelines for testing of chemicals.[53] Organs were harvested from mice that were administered with MCA-13 for the detection of possible toxicological lesions in the framework of a safety assessment. Organs (brain hyppocampus, heart, lung, stomach, kidneys, small intestine, colon, liver, spleen), of five HU-MCA-13 treated and three untreated mice, were harvested and fixed in 4% formaldehyde. Then, the organs were trimmed in a standard position per organ and put in embedding cassettes. (6 cassettes per organ per mice). Paraffin blocks were sectioned at approximately 3−5 μm thickness. The sections were applied on a glass slide and stained with hematoxylin and eosin. Pictures were taken on microscope (Olympus BX60) at magnification of X4 and X10 using microscope's Camera (Olympus DP73, serial NO. OH05504). The slides were examined by an experienced pathologist (Dr. Loeb Emanuel). Microscopic findings were classified with standard pathological nomenclature and severities of findings were graded on a scale of minimal, mild, or severe. Grades of severity for microscopic findings were subjective; minimal was the least extent discernible and severe was the greatest extent possible.

**DiscoverX's SAFETYscan methods.** Described in the Supporting Information.

**PhosphoSens CSox based kinase assays.** Described in the Supporting Information.

**Statistics.** Each experiment was performed in triplicates. Unless otherwise stated, by using SPSS software, one-way ANOVA was performed for the fractional dimension of each compound, in order to evaluate the neurotropic effect. In case of significance, Bonferroni post-hoc analysis was performed. The results were considered significant when $p < 0.01$.

## ■ ASSOCIATED CONTENT

### Supporting Information

The Supporting Information is available free of charge at https://pubs.acs.org/doi/10.1021/acschemneuro.0c00255.

Sensory motor/neurological performance; DiscoverX's SAFETY scan methods and individual target results; MCA-13 safety by in vitro evaluation using PhosphoSens CSoxbased kinase and phosphatase assays (PDF)

## ■ AUTHOR INFORMATION


### Corresponding Authors

**Dmitry Tsvelikhovsky** − *The Institute for Drug Research, Division of Medicinal Chemistry, School of Pharmacy, Faculty of Medicine, The Hebrew University of Jerusalem, Jerusalem 9112102, Israel;* orcid.org/0000-0002-1581-5291; Phone: (+972)2-675-7032; Email: dmitryt@ekmd.huji.ac.il; Fax: (+972)2-675-7076

**Philip Lazarovici** − *The Institute for Drug Research, Division of Pharmacology, School of Pharmacy, Faculty of Medicine, The Hebrew University of Jerusalem, Jerusalem 9112102, Israel;* Phone: (+972)2-675-8729; Email: philipl@ekmd.huji.ac.il; Fax: (+972)2-675-7490

### Authors

**Adi Lahiani** − *The Institute for Drug Research, Division of Pharmacology, School of Pharmacy, Faculty of Medicine, The Hebrew University of Jerusalem, Jerusalem 9112102, Israel*

**Dikla Haham-Geula** − *The Institute for Drug Research, Division of Pharmacology, School of Pharmacy, Faculty of Medicine, The Hebrew University of Jerusalem, Jerusalem 9112102, Israel*

**David Lankri** − *The Institute for Drug Research, Division of Medicinal Chemistry, School of Pharmacy, Faculty of Medicine, The Hebrew University of Jerusalem, Jerusalem 9112102, Israel*

**Susan Cornell-Kennon** − *AssayQuant Technologies Inc., Marlboro, Massachusetts 01752, United States*




https://dx.doi.org/10.1021/acschemneuro.0c00255
ACS Chem. Neurosci. 2020, 11, 2577−2589

**Erik M. Schaefer** − *AssayQuant Technologies Inc., Marlboro, Massachusetts 01752, United States*

Complete contact information is available at: https://pubs.acs.org/10.1021/acschemneuro.0c00255

### Author Contributions

Dmitry Tsvelikhovsky and Philip Lazarovici have directly participated in the conceptualization, supervision, data curation, formal analysis of the study, writing, reviewing and editing of the manuscript. Adi Lahiani, Dikla Haham-Geula, David Lankri, Susan Cornell-Kennon, Erik M. Schaefer: Methodology and Investigations. All authors have read and approved the final version submitted.

### Funding

D.T. holds the Gerald Heller Chair in Pharmaceutical Chemistry, gratefully acknowledge the Israel Science Foundation - ISF Research Grant (367/18) for the financial support. This work was also supported in part by the Hebrew University of Jerusalem - Yissum Intramural Research Funds. PL holds the Jacob Gitlin Chair in Physiology and is affiliated and supported by David R. Bloom Center for Pharmacy, Dr. Adolf and Klara Brettler Center for Research in Molecular Pharmacology and Therapeutics, and the Grass Center for Drug Design and Synthesis of Novel Therapeutics at the Hebrew University of Jerusalem, Israel.

### Notes

The authors declare no competing financial interest.

## REFERENCES

(1) Martyn, C. N., and Hughes, R. A. (1997) Epidemiology of peripheral neuropathy. *J. Neurol., Neurosurg. Psychiatry 62*, 310−318.
(2) Taylor, C. A., Braza, D., Rice, J. B., and Dillingham, T. (2008) The incidence of peripheral nerve injury in extremity trauma. *Am. J. Phys. Med. Rehabil. 87*, 381−385.
(3) Benarroch, E. E. (2015) Acquired axonal degeneration and regeneration: recent insights and clinical correlations. *Neurology 84*, 2076−2085.
(4) Barrell, K., and Smith, A. G. (2019) Peripheral Neuropathy. *Med. Clin. North Am. 103*, 383.
(5) (a) Landowski, L. M., Dyck, P. J. B., Engelstad, J., and Taylor, B. V. (2016) Axonopathy in peripheral neuropathies: Mechanisms and therapeutic approaches for regeneration. *J. Chem. Neuroanat. 76*, 19−27. (b) Brannagan, T. H., III (2012) Current issues in peripheral neuropathy. *J. Peripher. Nerv. Syst. 17*, 1−3.
(6) Cooper, D. J., Zunino, G., Bixby, J. L., and Lemmon, V. P. (2017) Phenotypic screening with primary neurons to identify drug targets for regeneration and degeneration. *Mol. Cell. Neurosci. 80*, 161−169.
(7) Skaper, S. D. (2005) Neuronal growth-promoting and inhibitory cues in neuroprotection and neuroregeneration. *Ann. N. Y. Acad. Sci. 1053*, 376−385.
(8) Compagnucci, C., Piemonte, F., Sferra, A., Piermarini, E., and Bertini, E. (2016) The cytoskeletal arrangements necessary to neurogenesis. *Oncotarget 7*, 19414−19429.
(9) Rocco, M. L., Soligo, M., Manni, L., and Aloe, L. (2018) Nerve growth factor: early studies and recent clinical trials. *Curr. Neuropharmacol. 16*, 1455−1465.
(10) Fletcher, J. L., Murray, S. S., and Xiao, J. (2018) Brain-derived neurotrophic factor in central nervous system myelination: a new mechanism to promote myelin plasticity and repair. *Int. J. Mol. Sci. 19*, 4131.
(11) Chang, H. J., Kim, H. J., and Chun, H. S. (2007) Quantitative structure− activity relationship (QSAR) for neuroprotective activity of terpenoids. *Life Sci. 80*, 835−841.
(12) Xiao, N., and Le, Q. T. (2016) Neurotrophic factors and their potential applications in tissue regeneration. *Arch. Immunol. Ther. Exp. 64*, 89−99.
(13) Wang, Y., Pan, J., Wang, D., and Liu, J. (2018) The Use of Stem Cells in Neural Regeneration: A Review of Current Opinion. *Curr. Stem Cell Res. Ther. 13*, 608−617.
(14) Lykissas, M. G., Batistatou, A. K., Charalabopoulos, K. A., and Beris, A. E. (2007) The role of neurotrophins in axonal growth, guidance, and regeneration. *Curr. Neurovasc. Res. 4*, 143−151.
(15) McArthur, J. C., Yiannoutsos, C., Simpson, D. M., Adornato, B. T., Singer, E. J., Hollander, H., Navia, B. A., et al. (2000) A phase II trial of nerve growth factor for sensory neuropathy associated with HIV infection. *Neurology 54*, 1080−1088.
(16) Fernandez, L., Komatsu, D. E., Gurevich, M., and Hurst, L. C. (2018) Emerging strategies on adjuvant therapies for nerve recovery. *J. Hand Surg. 43*, 368−373.
(17) (a) Calabrese, E. J. (2008) Enhancing and regulating neurite outgrowth. *Crit. Rev. Toxicol. 38*, 391−418. (b) Li, P., Matsunaga, K., Yamamoto, K., Yoshikawa, R., Kawashima, K., and Ohizumi, Y. (1999) Nardosinone, a novel enhancer of nerve growth factor in neurite outgrowth from PC12D cells. *Neurosci. Lett. 273*, 53−56.
(18) Al-Ali, H., Lee, D. H., Danzi, M. C., Nassif, H., Gautam, P., Wennerberg, K., Bixby, J. L., et al. (2015) Rational polypharmacology: systematically identifying and engaging multiple drug targets to promote axon growth. *ACS Chem. Biol. 10*, 1939−1951.
(19) Chaurasiya, N. D., Shukla, S., and Tekwani, B. L. (2017) A combined in vitro assay for evaluation of neurotrophic activity and cytotoxicity. *SLAS Discovery 22*, 667−675.
(20) Pankevich, D. E., Altevogt, B. M., Dunlop, J., Gage, F. H., and Hyman, S. E. (2014) Improving and accelerating drug development for nervous system disorders. *Neuron 84*, 546−553.
(21) Lankri, D., Haham, D., Lahiani, A., Lazarovici, P., and Tsvelikhovsky, D. (2018) Methylene-cycloalkylacetate (MCA) scaffold-based compounds as novel neurotropic agents. *ACS Chem. Neurosci. 9*, 691−698.
(22) (a) Marcos, I. S., Conde, A., Moro, R. F., Basabe, P., Díez, D., Mollinedo, F., and Urones, J. G. (2008) Synthesis of an ent-Halimanolide from ent-Halimic Acid. *Molecules 13*, 1120−1134. (b) Corey, E. J., and Roberts, B. E. (1997) Total synthesis of dysidiolide. *J. Am. Chem. Soc. 119*, 12425−12431. (c) Brown, G. D., Liang, G. Y., and Sy, L. K. (2003) Terpenoids from the seeds of Artemisia annua. *Phytochemistry 64*, 303−323. (d) Chiruvella, K. K., Mohammed, A., Dampuri, G., Ghanta, R. G., and Raghavan, S. C. (2007) Phytochemical and antimicrobial studies of methyl angolensate and luteolin-7-O-glucoside isolated from callus cultures of Soymida febrifuga. *Int. J. Biomed. Sci. 3*, 269−278.
(23) Tobal, I. E., Roncero, A. M., Moro, R. F., Díez, D., and Marcos, I. S. (2019) The Methylene-Cycloalkylacetate (MCA) Scaffold in Terpenyl Compounds with Potential Pharmacological Activities. *Molecules 24*, 2120.
(24) (a) Mostinski, Y., Valerio, V., Lankri, D., and Tsvelikhovsky, D. (2015) Synthesis of Tricyclic Spiranoid Lactones via $I_2$/Sm (II)-and $I_2$/Pd (0)-Mediated Cyclizations of a Common Cycloalkylmethylene Precursor. *J. Org. Chem. 80*, 10464−10473. (b) Valerio, V., Mostinski, Y., Kotikalapudi, R., and Tsvelikhovsky, D. (2016) Stereo-and Regioselective Synthesis of Tricyclic Spirolactones by Diastereoisomeric Differentiation of a Collective Key Precursor. *Chem. - Eur. J. 22*, 2640−2647.
(25) Fanarraga, M. L., Avila, J., and Zabala, J. C. (1999) Expression of unphosphorylated class III $\beta$-tubulin isotype in neuroepithelial cells demonstrates neuroblast commitment and differentiation. *Eur. J. Neurosci. 11*, 516−527.
(26) (a) Minnone, G., De Benedetti, F., and Bracci-Laudiero, L. (2017) NGF and its receptors in the regulation of inflammatory response. *Int. J. Mol. Sci. 18*, 1028. (b) Testa, G., Mainardi, M., Morelli, C., Olimpico, F., Pancrazi, L., Petrella, C., Strettoi, E., et al. (2019) The NGFR100W mutation specifically impairs nociception without affecting cognitive performance in a mouse model of

Hereditary Sensory and Autonomic Neuropathy type V. *J. Neurosci. 39*, 9702−9715.
(27) Burkey, T. H., Hingtgen, C. M., and Vasko, M. R. (2004). *Isolation and culture of sensory neurons from the dorsal-root ganglia of embryonic or adult rats*. Pain Research. Humana Press, 189−202.
(28) Kopić, A., Benamara, K., Schuster, M., Leidenmühler, P., Bauer, A., Glantschnig, H., and Höllriegl, W. (2019) Coagulation phenotype of wild-type mice on different genetic backgrounds. *Lab. Anim. 53*, 43−52.
(29) Otto, G. P., Rathkolb, B., Oestereicher, M. A., Lengger, C. J., Moerth, C., Micklich, K., and de Angelis, M. H. (2016) Clinical chemistry reference intervals for C57BL/6J, C57BL/6N, and C3HeB/FeJ mice (Mus musculus). *J. Am. Assoc. Lab. Anim. Sci. 55*, 375−386.
(30) Segall, M. D., and Barber, C. (2014) *Drug Discovery Today 19*, 688−693.
(31) Colerangle, J. B. (2017). Preclinical Development of Non-oncogenic Drugs (Small and Large Molecules). In *A Comprehensive Guide to Toxicology in Nonclinical Drug Development*. Academic Press, 659−683.
(32) Elgart, A., Cherniakov, I., Aldouby, Y., Domb, A. J., and Hoffman, A. (2013) Improved Oral Bioavailability of BCS Class 2 Compounds by Self Nano-Emulsifying Drug Delivery Systems (SNEDDS): The Underlying Mechanisms for Amiodarone and Talinolol. *Pharm. Res. 30*, 3029−3044.
(33) Smith, D. A., and Schmid, E. F. (2006) Drug withdrawals and the lessons within. *Curr. Opin. Drug. Disc. Dev. 9*, 38−46.
(34) Bowes, J., Brown, A. J., Hamon, J., Jarolimek, W., Sridhar, A., Waldron, G., and Whitebread, S. (2012) Reducing safety-related drug attrition: the use of in vitro pharmacological profiling. *Nat. Rev. Drug Discovery 11*, 909−922.
(35) Dambach, D. M., Misner, D., Brock, M., Fullerton, A., Proctor, W., Maher, J., Lee, D., Ford, K., and Diaz, D. (2016) Safety lead optimization and candidate identification: integrating new technologies into decision-making. *Chem. Res. Toxicol. 29*, 452−472.
(36) Karkoulias, G., and Flordellis, C. (2007) Delayed transactivation of the receptor for nerve growth factor is required for sustained signaling and differentiation by $\alpha$2-adrenergic receptors in transfected PC12 cells. *Cell. Signalling 19*, 945−957.
(37) (a) Zhang, F., Challapalli, S. C., and Smith, P. J. (2009) Cannabinoid CB1 receptor activation stimulates neurite outgrowth and inhibits capsaicin induced $Ca^{2+}$ influx in an in vitro model of diabetic neuropathy. *Neuropharmacology 57*, 88−96. (b) Asimaki, O., and Mangoura, D. (2011) Cannabinoid receptor 1 induces a biphasic ERK activation via multiprotein signaling complex formation of proximal kinases PKC$\epsilon$, Src, and Fyn in primary neurons. *Neurochem. Int. 58*, 135−144.
(38) Smalheiser, N. R., Dissanayake, S., and Kapil, A. (1996) Rapid regulation of neurite outgrowth and retraction by phospholipase A2-derived arachidonic acid and its metabolites. *Brain Res. 721*, 39−48.
(39) Yung, H. S., Chow, K. B., Lai, K. H., and Wise, H. (2009) Gi-coupled prostanoid receptors are the likely targets for COX-1-generated prostanoids in rat pheochromocytoma (PC12) cells. *Prostaglandins, Leukotrienes Essent. Fatty Acids 81*, 65−71.
(40) (a) Kim, H. S., Song, M., Kim, E., Ryu, S. H., and Suh, P. G. (2003) Dexamethasone differentiates NG108−15 cells through cyclooxygenase 1 induction. *Exp. Mol. Med. 35*, 203. (b) Choi, S. Y., Choi, B. H., Suh, B. C., Chae, H. D., Kim, J. S., Shin, M. J., Kim, K. T., et al. (2001) *J. Neurochem. 79*, 303−310.
(41) Hiruma, H., Ichikawa, T., Kobayashi, H., Hoka, S., Takenaka, T., and Kawakami, T. (2000) Prostaglandin E2 enhances axonal transport and neuritogenesis in cultured mouse dorsal root ganglion neurons. *Neuroscience 100*, 885−891.
(42) Kim, R. J., and Nam, J. S. (2011) OCT4 expression enhances features of cancer stem cells in a mouse model of breast cancer. *Lab. Anim. Res. 27* (2), 147−152.
(43) Sherman, S. P., and Bang, A. G. (2018) High-throughput screen for compounds that modulate neurite growth of human induced pluripotent stem cell-derived neurons. *Dis. Models & Mech. 11*, dmm031906.
(44) Peterson, L. B., Yaffe, M. B., and Imperiali, B. (2014) Selective mitogen activated protein kinase activity sensors through the application of directionally programmable D domain motifs. *Biochemistry 53*, 5771−5778.
(45) (a) Hagel, M., Miduturu, C., Sheets, M., Rubin, N., Weng, W., Stransky, N., Shutes, A., et al. (2015) First selective small molecule inhibitor of FGFR4 for the treatment of hepatocellular carcinomas with an activated FGFR4 signaling pathway. *Cancer Discovery 5* (4), 424−437. (b) Planken, S., Behenna, D. C., Nair, S. K., Johnson, T. O., Nagata, A., Almaden, C., Cho-Schultz, S., et al. (2017) Discovery of N-((3 R, 4 R)-4-Fluoro-1-(6-((3-methoxy-1-methyl-1 H-pyrazol-4-yl) amino)-9-methyl-9 H-purin-2-yl) pyrrolidine-3-yl) acrylamide (PF-06747775) through Structure-Based Drug Design: A High Affinity Irreversible Inhibitor Targeting Oncogenic EGFR Mutants with Selectivity over Wild-Type EGFR. *J. Med. Chem. 60*, 3002−3019. (c) Cheng, H., Nair, S. K., Murray, B. W., Almaden, C., Bailey, S., Baxi, S., Edwards, M. P., et al. (2016) Discovery of 1-{(3 R, 4 R)-3-[({5-Chloro-2-[(1-methyl-1 H-pyrazol-4-yl) amino]-7 H-pyrrolo [2, 3-d] pyrimidin-4-yl} oxy) methyl]-4-methoxypyrrolidin-1-yl} prop-2-en-1-one (PF-06459988), a Potent, WT Sparing, Irreversible Inhibitor of T790M-Containing EGFR Mutants. *J. Med. Chem. 59*, 2005−2024.
(46) Jang, S. W., Okada, M., Sayeed, I., Xiao, G., Stein, D., Jin, P., and Ye, K. (2007) Gambogic amide, a selective agonist for TrkA receptor that possesses robust neurotrophic activity, prevents neuronal cell death. *Proc. Natl. Acad. Sci. U. S. A. 104*, 16329−16334.
(47) Meberg, P. J., Ono, S., Minamide, L. S., Takahashi, M., and Bamburg, J. R. (1998) Actin depolymerizing factor and cofilin phosphorylation dynamics: response to signals that regulate neurite extension. *Cell Motil. Cytoskeleton 39*, 172.
(48) Katzir, I., Shani, J., Regev, K., Shabashov, D., and Lazarovici, P. (2002) A quantitative bioassay for nerve growth factor, using PC12 clones expressing different levels of trkA receptors. *J. Mol. Neurosci. 18*, 251−264.
(49) Arien-Zakay, H., Lecht, S., Perets, A., Roszell, B., Lelkes, P. I., and Lazarovici, P. (2009) Quantitative assessment of neuronal differentiation in three-dimensional collagen gels using enhanced green fluorescence protein expressing PC12 pheochromocytoma cells. *J. Mol. Neurosci. 37*, 225−237.
(50) Filous, A. R., and Silver, J. (2016) Neurite outgrowth assay. *Bio Protoc. 6*, e1694.
(51) Das, M., Bhargava, N., Bhalkikar, A., Kang, J. F., and Hickman, J. J. (2008) Temporal neurotransmitter conditioning restores the functional activity of adult spinal cord neurons in long-term culture. *Exp. Neurol. 209*, 171−180.
(52) Momic, T., Katzehendler, J., Benny, O., Lahiani, A., Cohen, G., Noy, E., Lazarovici, P., et al. (2014) Vimocin and vidapin, cyclic KTS peptides, are dual antagonists of $\alpha1\beta1/\alpha2\beta1$ integrins with antiangiogenic activity. *J. Pharmacol. Exp. Ther. 350*, 506−519.
(53) Chemicals, D. O. F. O. *OECD Guideline for testing of chemicals*. The Organisation for Economic Co-operation and Developmen. (2005). Paris, France, 1−13.


https://dx.doi.org/10.1021/acschemneuro.0c00255
*ACS Chem. Neurosci.* 2020, 11, 2577−2589